Acta Pharmaceutica Sinica B 2025;15(6):3149−3162



Chinese Pharmaceutical Association
Institute of Materia Medica, Chinese Academy of Medical Sciences

Acta Pharmaceutica Sinica B

www.elsevier.com/locate/apsb
www.sciencedirect.com



ORIGINAL ARTICLE

Psychological stress-activated NR3C1/NUPR1 axis promotes ovarian tumor metastasis



Bin Liu[a,b,c], Wen-Zhe Deng[b,c,d], Wen-Hua Hu[e], Rong-Xi Lu[e], Qing-Yu Zhang[f], Chen-Feng Gao[a], Xiao-Jie Huang[a], Wei-Guo Liao[e], Jin Gao[c], Yang Liu[b,c], Hiroshi Kurihara[b,c], Yi-Fang Li[b,c,g], Xu-Hui Zhang[g,*], Yan-Ping Wu[b,*], Lei Liang[b,*], Rong-Rong He[b,c,g,*]

[a]*Laboratory of Hepatobiliary Surgery, Zhanjiang Key Laboratory of Hepatobiliary Related Diseases, Affiliated Hospital of Guangdong Medical University, Zhanjiang 524001, China*
[b]*State Key Laboratory of Bioactive Molecules and Druggability Assessment, Guangdong Basic Research Center of Excellence for Natural Bioactive Molecules and Discovery of Innovative Drugs, Guangdong Engineering Research Center of Traditional Chinese Medicine & Disease Susceptibility, Guangdong Engineering Research Center of Traditional Chinese Medicine & Health Products, International Cooperative Laboratory of TCM Modernization and Innovative Drug Development of Chinese Ministry of Education (MOE), Guangdong Province Key Laboratory of Pharmacodynamic Constituents of TCM and New Drugs Research, Jinan University, Guangzhou 510632, China*
[c]*College of Pharmacy, Jinan University, Guangzhou 510632, China*
[d]*Department of Pharmacy, Shaoguan First People's Hospital, Shaoguan 512000, China*
[e]*Pathology Diagnosis and Research Center, the Affiliated Hospital of Guangdong Medical University, Zhanjiang 524001, China*
[f]*Laboratory of Obstetrics and Gynecology, Department of Obstetrics and Gynecology, the Affiliated Hospital of Guangdong Medical University, Zhanjiang 524001, China*
[g]*Department of Oncology, Guangdong Second Provincial General Hospital, the Affiliated Guangdong Second Provincial General Hospital of Jinan University, Guangzhou 510317, China*

Received 27 June 2024; received in revised form 30 September 2024; accepted 20 December 2024

KEY WORDS

NR3C1;
NUPR1;
Ovarian tumor;

Abstract Ovarian tumor (OT) is the most lethal form of gynecologic malignancy, with minimal improvements in patient outcomes over the past several decades. Metastasis is the leading cause of ovarian cancer-related deaths, yet the underlying mechanisms remain poorly understood. Psychological stress is known to activate the glucocorticoid receptor (NR3C1), a factor associated with poor prognosis in OT patients. However, the precise mechanisms linking NR3C1 signaling and metastasis have yet to be fully

*Corresponding authors.
E-mail addresses: rongronghe@jnu.edu.cn (Rong-Rong He), leiliang@jnu.edu.cn (Lei Liang), wuyanping@jnu.edu.cn (Yan-Ping Wu), zhangxh@gd2h.org.cn (Xu-Hui Zhang).

Peer review under the responsibility of Chinese Pharmaceutical Association and Institute of Materia Medica, Chinese Academy of Medical Sciences.

https://doi.org/10.1016/j.apsb.2025.04.001
2211-3835 © 2025 The Authors. Published by Elsevier B.V. on behalf of Chinese Pharmaceutical Association and Institute of Materia Medica, Chinese Academy of Medical Sciences. This is an open access article under the CC BY-NC-ND license (http://creativecommons.org/licenses/by-nc-nd/4.0/).

EMT;
Prognostic biomarker;
Psychological stress;
Therapeutic target;
SNAI2

elucidated. In this study, we demonstrate that chronic restraint stress accelerates epithelial−mesenchymal transition (EMT) and metastasis in OT through an NR3C1-dependent mechanism involving nuclear protein 1 (NUPR1). Mechanistically, NR3C1 directly regulates the transcription of NUPR1, which in turn increases the expression of snail family transcriptional repressor 2 (SNAI2), a key driver of EMT. Clinically, elevated NR3C1 positively correlates with NUPR1 expression in OT patients, and both are positively associated with poorer prognosis. Overall, our study identified the NR3C1/NUPR1 axis as a critical regulatory pathway in psychological stress-induced OT metastasis, suggesting a potential therapeutic target for intervention in OT metastasis.

© 2025 The Authors. Published by Elsevier B.V. on behalf of Chinese Pharmaceutical Association and Institute of Materia Medica, Chinese Academy of Medical Sciences. This is an open access article under the CC BY-NC-ND license (http://creativecommons.org/licenses/by-nc-nd/4.0/).

1. Introduction

Epidemiological studies indicate that ovarian tumor (OT) is among the most lethal gynecological malignancies, ranking as the eighth leading cause of death among women worldwide[1]. The incidence of ovarian cancer continues to rise annually[2] and OT patients frequently exhibit poor responses to standard chemotherapy regimens[3]. As a result, the identification of novel biomarkers and therapeutic targets is urgently needed to improve clinical outcomes for these patients. Research suggests that OT patients who experience adverse life events and chronic anxiety during the first year after diagnosis are more likely to face poor prognosis[4]. Moreover, symptoms of anxiety and depression triggered by psychological stress, including various social pressures, have been shown to accelerate the progression of OT[5].

Recent studies have shown that elevated stress hormone levels during breast cancer progression activate the glucocorticoid receptor (NR3C1) at distant metastatic sites, leading to increased colonization and reduced survival rates[6]. Accumulating evidence suggests that psychological stress may also promote the progression and metastasis of various cancers, including OT and hepatocellular carcinoma[7,8]. Epidemiological studies have linked dysregulated stress hormone cortisol levels with shorter survival in OT patients[4]. Additionally, psychological stress has been reported to decrease serotonin levels in the ovary, thereby enhancing OT growth in mice[9]. Stress hormones have also been found to regulate interleukin-6 expression in human ovarian carcinoma cells *via* a Src-dependent mechanism[10]. Psychological stress activates the hypothalamic−pituitary−adrenal axis, leading to the release of multiple hormones including glucocorticoid (GC, cortisol in humans, corticosterone in rodents), which influences systemic physiology[7,11]. Emerging evidence from the hormone-omics analysis in our recently published research further revealed that corticosterone (CORT) was the most significantly increased hormone in mice subjected to stress[12,13]. GC exerts its effects by binding to NR3C1, inducing its translocation into the nucleus, where NR3C1 functions as a transcription factor that either positively or negatively regulates the expression of GC-responsive genes[14]. Furthermore, GC has been shown to reduce the effectiveness of chemotherapy in cell lines and xenograft models of several types of solid tumors, including breast cancer[15], pancreatic cancer[16], and ovarian carcinoma[17]. Notably, NR3C1 expression has been detected in 88% of ovarian tumors[18] and high NR3C1 expression is associated with shorter progression-free survival (PFS) in OT patients[19]. However, the specific mechanism by which chronic stress affects OT invasion and metastasis through NR3C1 remains elusive.

Epithelial−mesenchymal transition (EMT), is a critical step in tumor progression, facilitating the transition from tumor initiation to metastasis[20,21]. This process involves alterations in cytoskeletal proteins and reduced cell adhesion, which enhance cellular migration and invasion capabilities. Previous studies have shown that *SNAI2* was significantly increased in metastatic ovarian cancer cells[22]. Besides, NR3C1 activation can regulate the promoter of *SNAI2*, which in turn reduces the E-cadherin (CDH1) level, thereby promoting cell invasion and metastasis[23-25]. However, the precise mechanism by which NR3C1 regulates EMT remains unclear. Amount researches suggest that there is a bidirectional and intricate relationship between NR3C1 and estrogen receptor[26-29], which plays a significant role in nuclear protein 1 (NUPR1) regulation, as supported by existing literature[30]. This association underscores the potentially intricate linkage between NR3C1 and NUPR1, highlighting the potential for cross-regulatory mechanisms within this signaling network. NUPR1, a stress-responsive factor, has been shown to play various roles in cellular stress responses, including involvement in endoplasmic reticulum (ER) stress[31]. Given its diverse roles in cancer, NUPR1 has attracted significant attention, with several studies focused on identifying its molecular targets and developing potential cancer therapies[32]. For example, transcriptional co-regulator NUPR1 has been implicated in tamoxifen resistance in breast cancer[30], and inhibition of NUPR1 translocation from cytoplasm to nucleus has been shown to increase the sensitivity of pancreatic cancer cells to genotoxic drugs[33,34]. Furthermore, NUPR1 deficiency has been linked to delayed ovarian maturation and ovarian follicular atresia in pigs[35]. Despite these findings, the role and molecular mechanisms of NUPR1 in the development and progression of OT remain largely unexplored.

In this study, we identified the NR3C1−NUPR1 axis as a crucial pathway through which psychological stress accelerates the growth and metastasis of OT. This connection between stress and cancer progression is well-known, but our study is the first to reveal how NR3C1 directly regulates NUPR1 to drive EMT. These findings add a new layer to the understanding of stress-related cancer biology by pinpointing specific molecular interactions that can be targeted for therapeutic intervention. Additionally, we validated our results with clinical OT samples, showing that elevated levels of NR3C1 and NUPR1 correlate with poor patient outcomes. This underscores the clinical relevance of our work and suggests that the disrupted NR3C1−NUPR1 pathway could offer new treatment options for OT patients, particularly those whose conditions are exacerbated by stress.

2. Materials and methods

2.1. Cell culture, transfection, and stable cell line construction

Human ovarian tumor cell lines, including SKOV3 cells and A2780 cells, were obtained from the American Type Culture Collection (Rockville, MD). HO8910 cells and ID8-Luc cells were purchased from the Chinese Academy of Sciences (Shanghai, China) and YUCHI Biology (Shanghai, China). All cell lines are authenticated by STR profiling. A2780 cells and ID8-Luc cells were cultured in DMEM, whereas SKOV3 cells and HO8910 cells were cultured in McCoy's 5A. All media were supplemented with 10% Fetal Bovine Serum (Gibco, Grand Island, NY, USA), 50 units/mL penicillin/streptomycin. Cells were kept in a humidified incubator at 37 °C with 5% CO_2. Transfections were performed by Lipofectamine 2000 Transfection Reagent (Invitrogen, Carlsbad, CA, USA), and siRNA transfections were performed with Lipofectamine RNAi-MAX (Life Technologies, Carlsbad, CA, USA) in the antibiotics-free medium according to manufacturer instructions. Infected cells were subsequently collected for polymerase chain reaction (PCR) and Western blot (WB) analysis. To construct the SKOV3-GFP-Luc stable cell line, the puro-GFP-Luc plasmid was packaged using lentivirus (TransGen Biotech, Beijing, China), and the procedures were conducted according to the manufacturer's protocol (Life Technologies). After approximately 2 weeks of screening, fluorescence imaging confirmed the successful establishment of the SKOV3-GFP-Luc stable cell line.

2.2. Animals and treatment

Female C57BL/6J mice (4−6 weeks old) and female nude mice (5 weeks old) were purchased from Laboratory Animal Center of Southern Medical University and Shanghai Laboratory Animal Center, respectively. All mice were maintained in a temperature-controlled room with a 12 h light/dark cycle and adaptive feed for a week before experiments. Animal protocols were approved by the Institutional Animal Care and Use Committee (No. AHGDMU-LAC-B-2023-08-0061). All mice received humane care according to the criteria outlined in the "Guide for the care and use of laboratory animals".

In the first batch of animal experiments, an orthotopic ovarian cancer model was established in C57BL/6 mice, following previously published methods[36]. Briefly, mice were anesthetized with 5% isoflurane (RWD Life Science, Shenzhen, China) using an animal anesthetic machine (Shanghai Yuyan Instruments Co., Ltd., Shanghai, China), with anesthesia maintained at 2% isoflurane throughout the procedure. Mice were immobilized in a prone position, and a 0.5 cm longitudinal incision was made to the left of the dorsal midline. The ovary was carefully clamped with forceps and injected with 10 μL of ID8-Luc cell suspension using a fine needle. After a 5-s absorption period, the ovary was repositioned, and the skin was meticulously sutured using absorbable thread. Mice were then returned to their cage to recover for 1 week. The orthotopic ovarian cancer model mice were randomly divided into 2 groups: the control group and the stress group. Mice in the stress group received a daily 6 h-restraint stress (4:00 pm to 10:00 pm) in a polypropylene tube with ventilation holes for 6 weeks. Body weight was measured weekly for all mice.

In the second batch of animal experiments, female nude mice were randomly divided into 4 groups: control, stress, corticosterone (CORT, Sigma−Aldrich, Saint Louis, MO, USA), and stress + Ru486 (an antagonist of NR3C1, mifepristone (Sigma−Aldrich)). Mice in the stress group received a 2 h-restraint stress (6:00 pm to 8:00 pm) daily in a polypropylene restraint tube with holes for 30 days. Mice in the CORT group were daily subcutaneously injected with CORT (1 mg/kg) for 30 days. Mice in the stress + Ru486 group received 30 days of Ru486 (25 mg/kg, subcutaneous injection, daily) before restraint loading (Supporting Information Fig. S1A). The dosage of Ru486 and CORT were administered according to our previous research[13,37]. After 2 days of restraint stress, Ru486 or CORT treatment, a total number of 5×10^6 SKOV3-GFP-Luc cells were intraperitoneally injected into each nude mouse, and the body weight was monitored every day.

The tumor metastasis in mice was imaged using an *in vivo* imaging system (IVIS-100 Spectrum, PerkinElmer, Waltham, MA, USA) after 7 weeks (in the first batch of animal experiments) or 22 days (in the second batch of animal experiments) of implantation. Tumor tissues were fixed in 4% paraformaldehyde and embedded in paraffin, and the whole blood was collected to detect the CA125 and corticosterone.

2.3. Determination of corticosterone in serum

Serum samples were collected from mice, and cortisone was added as an internal standard. Methyl *tert*-butyl ether was then added to the serum and thoroughly mixed using a vortex mixer. The upper layer was separated and dried by nitrogen gas. The dried sample was reconstituted in methanol and centrifugated at 14,000 × *g* for 25 min. The supernatant was collected for further analysis. Corticosterone concentration in the serum was quantified using liquid chromatography coupled with tandem mass spectrometry. The chromatographic separation was carried out on a vanquish high-performance liquid chromatography system paired with a Q-exactive high-resolution mass spectrometer. Separation was achieved using a Hypersil GOLD column (50 mm × 2.1 mm, 1.9 μm) with a mobile phase consisting of 0.1% formic acid in water (A) and acetonitrile (B). The elution gradient was as follows: 0−3 min, 27% B; 3−9 min, 27% B to 43% B; 9−14 min, 43% B to 53% B; 14−14.5 min, 53% B to 95% B; 14.5−18.5 min, 95% B; 18.5−19 min, 95% B to 27% B; 19−23 min, 27% B. The flow rate was maintained at 0.25 mL/min, with the column temperature set at 35 °C, and an injection volume of 2 μL. Mass spectrometry analysis was performed in positive ion mode, scanning a mass-to-charge (*m*/z) range of 150−1000 at a resolution of 70,000, with a maximum injection time of 100 ms. Key instrument settings included a capillary spray voltage of 3.5 kV, a capillary temperature of 320 °C, an auxiliary gas heater temperature of 350 °C, and an S-lens RF level of 65.

2.4. MTT assay for cell proliferation

The SKOV3, HO8910, and A2780 cell lines were seeded into 96-well plates at a density of 5000 cells/well. Subsequently, the cells were treated with or without cortisol for the specified duration. Following the treatment, MTT reagent (Beyotime Biotechnology, Shanghai, China) was added to each well for an additional 4 h. After removing the supernatant, the cells were lysed in DMSO for 10 min, and the optical density of each well was measured using a microplate reader (ThermoFisher Scientific, Waltham, MA, USA) at an absorbance of 450 nm.

2.5. Wound-closure, invasion, and migration assay

Cells (10^5 cells/well) were seeded in 6-well culture plates and cultured until they grew confluent. A straight scratch was

generated using a pipette tip to simulate a wound, and then the average distance from the edge to the center was measured at the designated time. Transwell Permeable Supports (inserts of 6.5 mm in diameter; Corning, Somerville, MA, USA) with 8 μm pores were used for cell invasion and migration assays. BD Bio Coat Matrigel Invasion Chamber (BD Biosciences, East Rutherford, NJ, USA) was used for a cell invasion assay. Cell suspension in normal medium was added to the upper chamber at various densities depending on the cell line. After the cells were attached to the dish, serum-free medium mixed with/without CORT was added to the lower chamber to act as an attractant. Cells were then incubated in normal culture conditions for 24 h. After incubation, migrated or invaded cells were fixed with methanol for 30 min and stained with 1 × crystal violet. Cells were counted in five randomly selected fields and photographed for each chamber.

2.6. Genome-wide expression profiling analysis

Total RNA from SKOV3 cells treated with/without cortisol for 24 h was extracted and then reverse transcribed to cDNA. Then the cDNA was processed using the Affymetrix gene chip fluidic station 450 (protocol EukGE-WS2v5_450; Santa Clara, CA, USA) and scanned using a Gene chip scanner 3000 G7 (Affymetrix). The gene chip operating software (Affymetrix GCOS v1.4) was used to obtain chip images with quality control conducted using the AffyQC report software. The original data were normalized by the limma package in the R software. The Kyoto Encyclopedia of Genes and Genomes (KEGG) pathway enrichment and the Gene Ontology (GO) function enrichment, the heatmap of differentially expressed genes (fold-change ≥ 2; $P \leq 0.05$) was plotted by https://www.bioinformatics.com.cn, an online platform for data analysis and visualization.

2.7. Quantitative polymerase chain reaction (qPCR) analysis

RNA isolation, cDNA synthesis, and real-time qPCR Detecting System, qPCR were performed as described previously, according to the manufacturer's protocol[38]. PCR oligo sequences for human samples are shown in Supporting Information Table S1 and qPCR was performed as described previously[39]. Relative mRNA expression of each gene was normalized with housekeeping gene through the delta cycle threshold method.

2.8. Western blot analysis

Total cell protein was extracted as described previously[39]. The extracted protein was subjected to sodium dodecyl sulfate-polyacrylamide gel electrophoresis. Primary antibodies used were as follows: NR3C1 (#12041), SNAI2 (#9585), CDH1 (#3195), GAPDH (#2118) (Cell Signaling Technologies, Danvers, MA, USA), and NUPR1 (ab6028, Abcam, Cambridge, UK).

2.9. Immunofluorescence assay

Ovarian tumor cells cultured in a glass dish were fixed with 4% paraformaldehyde and permeabilized with 0.2% Triton X-100. After blocked with 10% goat serum, the cells were incubated with primary antibodies (NR3C1 or NUPR1) at 4 °C overnight. The cell dish was then incubated with fluorescent secondary antibodies (#4417, Cell Signaling Technologies) for 1 h at room temperature, and then the nucleus was stained with DAPI (C1002, Beyotime Biotechnology). Lastly, cells were observed with a laser scanning confocal microscope (TCS SP5 II, LEICA, Mannheim, Germany).

2.10. Luciferase reporter assay

Cells were seeded into a 48-well plate and subsequently transfected with NUPR1-promoter luciferase reporter plasmids, pRL-TK vector (serving as an internal control with *Renilla* luciferase gene), and *NR3C1* plasmids. The transfection procedure utilized DNA transfection reagent from Neofect Biotech (Beijing, China), following the manufacturer's protocols. The following day, the culture medium was replaced, either with or without cortisol. Luciferase activities were assessed using the dual-luciferase reporter assay system in conjunction with the GloMax 20/20 luminometer (Promega Corporation, Madison, WI, USA). The resulting relative luciferase activity values were then normalized to the control group.

2.11. Chromatin immunoprecipitation

Chromatin immunoprecipitation (ChIP) assays were performed using the enzymatic chromatin IP kit (Cell Signaling Technologies). In brief, cells were cross-linked in 37% formaldehyde for 10 min and the reaction was quenched by glycine. After cell lysis, the nuclei were treated with micrococcal nuclease for digestion. The resulting sheared chromatin was then subjected to immunoprecipitation with antibodies against NR3C1 or normal IgG (#2729, Cell Signaling Technologies) as the control. Subsequently, the immunoprecipitated chromatin was decross-linked at 65 °C for 4 h, followed by purification using spin columns. The purified DNAs were subjected to analysis *via* qPCR using specific primers.

2.12. Patient specimens

The paraffin-embedded tissue came from 75 women diagnosed with ovarian tumor, 9 women diagnosed with ovarian endometrial cysts (OC) and 5 women diagnosed with hysteromyoma at Affiliated Hospital of Guangdong Medical University between 2014 and 2018. Inclusion criteria: patients with uterine fibroids: diagnosed with uterine fibroids and no lesions in ovarian tissue, treatment of uterine and ovarian tissue has been completed (surgical removal). Patients with ovarian tumors: diagnosed with primary ovarian tumor, treatment (surgery) of the primary tumor has been completed. Patients with endometriotic ovarian cysts: diagnosed with endometriotic ovarian cysts, endometriotic ovarian cysts have completed treatment (surgery). Exclusion criteria: patients who have been treated or have other active cancers; history of cardiovascular disease; history of mental illness; patients who have long-term diseases or are taking foods and drugs that may change the activity of the nervous system. None of the patients received chemotherapy or radiotherapy before surgical resection, and all specimens were obtained during the initial surgery. The work described has been carried out in accordance with the code of ethics of the World Medical Association (Declaration of Helsinki) for experiments involving humans. Ethical approval was granted by the Ethics Committee of the Affiliated Hospital of Guangdong Medical University (No. PJ2019-012). Clinicopathologic variables data and magnetic resonance imaging for all eligible patients were obtained from electronic medical records.

2.13. Immunohistochemistry analysis

Formalin-fixed and paraffin-embedded tissue were processed into 4 μm sections, and then Immunohistochemistry (IHC) was performed according to the manufacturer's protocol[39]. The antibodies used were NR3C1 and NUPR1 (1:200, orb101189, Biorbyt, Cambridge, UK). The density of NR3C1 and NUPR1 staining in each specimen was scored according to the number of positively stained cells (200 ×). The scoring standard was as follows: (0 points for no cells stained, 1 point for <10%, 2 points for 11%−50%, 3 points for 51%−80%, and 4 points for >80% of cells stained). The intensity of NR3C1 and NUPR1 immunostaining was scored as 1, 2, and 3 for weak, moderate, and strong immunoreactivity, respectively. The immunoreactivity score (IRS) resulted from the multiplication of both parameters. The final score of specimens was classified as follows: negative (IRS = 0), low (IRS = 1−6), and high (IRS = 7−12).

2.14. Statistical analysis

Data are presented as the mean ± standard deviation (SD) from at least 3 independent experiments. *P* values were determined using two-tailed *t*-test for comparison between 2 groups or one-way analysis of variance (ANOVA) for comparison of more than 2 groups by GraphPad Prism. Clinicopathological analysis was analyzed with the SPSS 19.0 (IBM Corporation). Statistical significance was assigned as $*P < 0.05$, $**P < 0.01$, and $***P < 0.001$.

3. Results

3.1. Psychological stress-evoked OT metastasis is mediated by NR3C1 activation

To investigate the effects of psychological stress on OT, mice were orthotopically injected with ID8-Luc cells and subjected to 6 h of daily chronic restraint stress for 6 weeks (Fig. 1A). As a result of stress, CA125 levels (a known OT marker[40]), tumor weight and tumor volume were significantly increased in restraint stress mice compared to control mice (Fig. 1B−E). Living imaging analysis further revealed that restraint stress remarkably accelerated OT metastasis in mice (Fig. 1F and G). Histopathological analysis confirmed that mice suffering from restraint stress exhibited a greater number of metastatic foci in the intestine, peritoneum, and diaphragm (Fig. 1H−M). In line with our previous findings that corticosterone, a typical stress-induced hormone GC in rodents, contributes to the activation of NR3C1[13,37], serum corticosterone levels and NR3C1 activation in OT tissues were both elevated in restraint-stressed mice (Fig. 1N−P). To verify that restraint stress-induced NR3C1 activation contributes to stress-provoked OT metastasis, SKOV3-GFP-Luc cells-inoculated nude mice were daily administered with CORT and NR3C1 antagonist mifepristone (Ru486) (Fig. S1A). As expected, both corticosterone and CA125 levels in serum were significantly increased in stressed and CORT-treated mice, whereas Ru486 treatment blocked the stress-induced rise in CA125 level (Fig. S1B and S1C). *In vivo* imaging results also demonstrated that OT metastasis was obviously enhanced by CORT treatment, similar to the effect of restraint stress. However, stress-induced OT metastasis was inhibited by Ru486 treatment (Fig. 1Q, Fig. S1D). Besides, NR3C1 activation in OT tissue was elevated in both stressed and CORT-treated mice, while Ru486 effectively prevented this activation (Fig. S1E). Taken together, these results confirm that psychological stress-evoked OT metastasis is linked to GC-induced NR3C1 activation.

3.2. NR3C1 activation contributes to the invasion and migration of OT

Subsequently, we investigated the potential role of NR3C1 activation in the invasion and metastasis of OT cells *in vitro*. Considering the higher expression levels of NR3C1 in SKOV3 and HO8910 cells (Fig. 2A), these cells were chosen for this study. The effect of cortisol at various concentrations on cell growth was examined by MTT assay. As shown in Fig. 2B and Supporting Information Fig. S2A, cortisol did not significantly affect the growth of SKOV3 or HO8910 cells, even at concentrations as high as 50 μmol/L. Interestingly, treatment with cortisol induced notable morphological changes in these cells, including spindle shape, loose cell connections, and invadopodium formation. These changes were partially reversed by Ru486 (Fig. 2C). Wound-healing and chamber assay further revealed that cortisol significantly enhanced the migratory ability of SKOV3 and HO8910 cells in a time-dependent manner, which could be blocked by Ru486 (Fig. 2D and F, Fig. S2B). Similarly, cortisol increased the invasive capabilities of OT cells, which were mitigated by Ru486 (Fig. 2E and F, Fig. S2C and S2D). Further, we silenced the expression of NR3C1 *in vitro* using its specific siRNAs (Fig. S2E). Consistently, the nuclear localization of NR3C1 in response to cortisol was dramatically decreased in cells transfected with *NR3C1* siRNA (Fig. 2G, Fig. S2F). Aside from that, *NR3C1* knockdown significantly diminished the migration and invasion activities of cortisol-treated OT cells (Fig. 2H and I). These findings suggest that NR3C1 activation contributes to the invasion and migration of OT.

3.3. NUPR1 expression is highly correlated with GC-induced NR3C1 activation

To identify the molecular mechanisms by which NR3C1 activation regulates OT metastasis, we conducted expression profile chip analysis on SKOV3 cells treated with GC. The top 15 KEGG pathway enrichment analysis among the differential expressed genes included the pathway in cancer, focal adhesion, and transcriptional misregulation in cancer (Fig. 3A). The heatmap highlights the differential genes expression related to the above pathways (Fig. 3B). It is noted that NUPR1, a gene involved in the pathway of transcriptional misregulation in cancer, was significantly upregulated in GC-treated SKOV3 cells. Aside from that, the top 15 enriched biological processes, such as response to hormones, positive regulation of cell migration, and regulation of cell−cell adhesion, were visualized in a bubble diagram (Fig. 3C). The GO chord diagram shows overlapping differential genes, including *NUPR1*, *SNAI2*, *CDH1,* across these biological processes (Fig. 3D). As anticipated, qPCR and Western blot analysis confirmed that both mRNA and protein expression levels of NUPR1 and SNAI2 in GC-treated SKOV3 cells were significantly upregulated (Fig. 3E−G). The correlation of *NR3C1* mRNA level and *NUPR1* mRNA level in human OT samples from TCGA PanCancer Atlas further confirmed a positive correlation between *NR3C1 and NUPR1* in the progression of OT (Fig. 3H). These

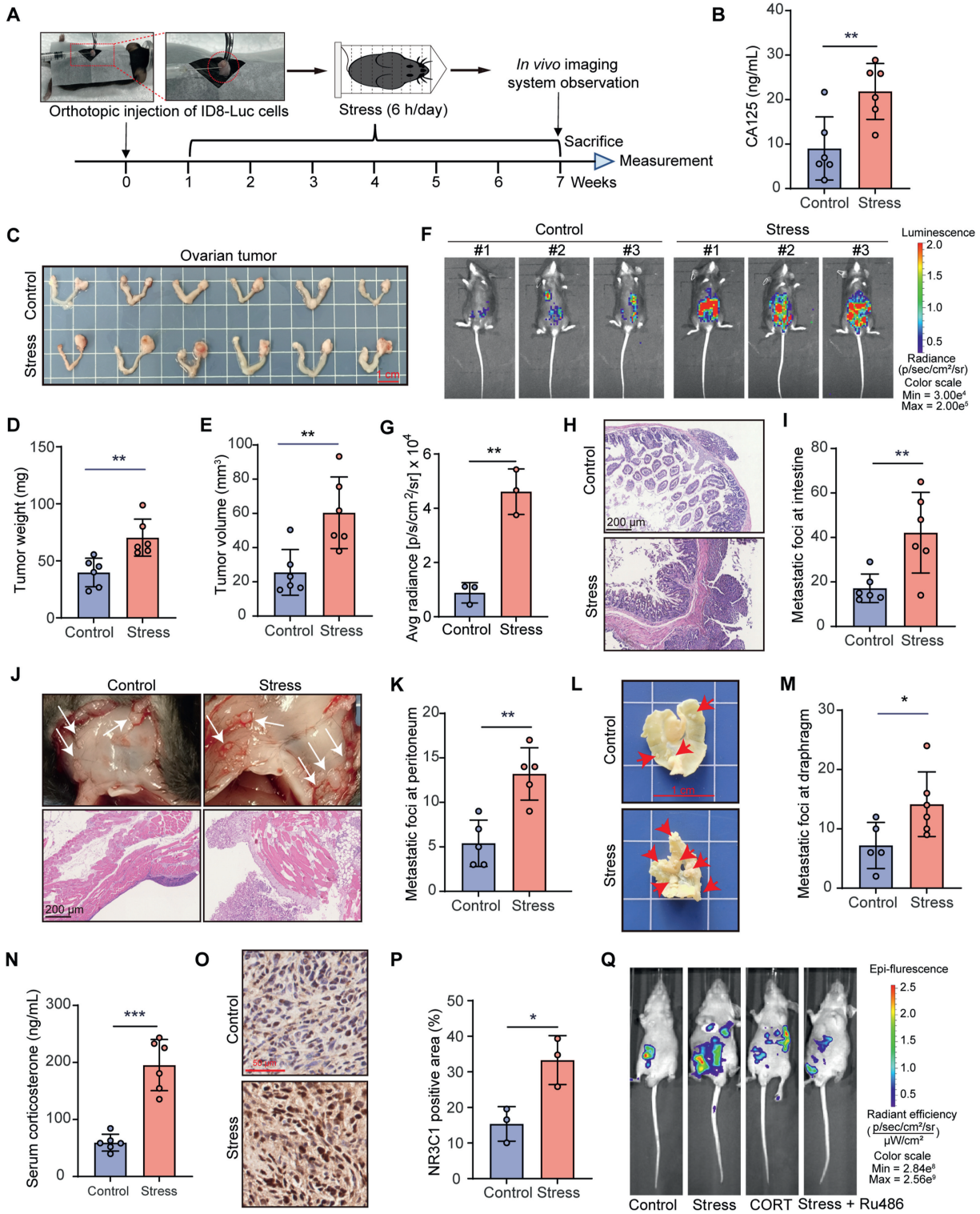


Figure 1 Psychological stress-evoked OT metastasis is mediated by NR3C1 activation. (A) Time course of the experimental procedure. Mice were orthotopically injected with ID8-Luc cells, and then exposed to restraint stress daily for 6 weeks. (B−E) The OT marker CA125, tumor photograph, tumor weight, and tumor volume were measured on the 7th week ($n = 6$). (F, G) The OT metastasis *in vivo* was imaged by a living imaging system, and the luminescence intensity was quantified ($n = 3$). Metastatic foci at (H, I) intestine, (J, K) peritoneum and (L, M) diaphragm in mice were measured and quantified ($n = 5$−6). (N) The corticosterone level from the serum of mice was detected by LC/MS ($n = 6$). (O, P) The activation of NR3C1 in OT tissue was measured by IHC ($n = 3$). (Q) Representative fluorescence imaging of OT metastasis in mice treated with Stress, CORT, and Stress + Ru486 ($n = 3$). All data represent mean ± SD. $^*P < 0.05$, $^{**}P < 0.01$, $^{***}P < 0.001$, by independent-samples *t* test.

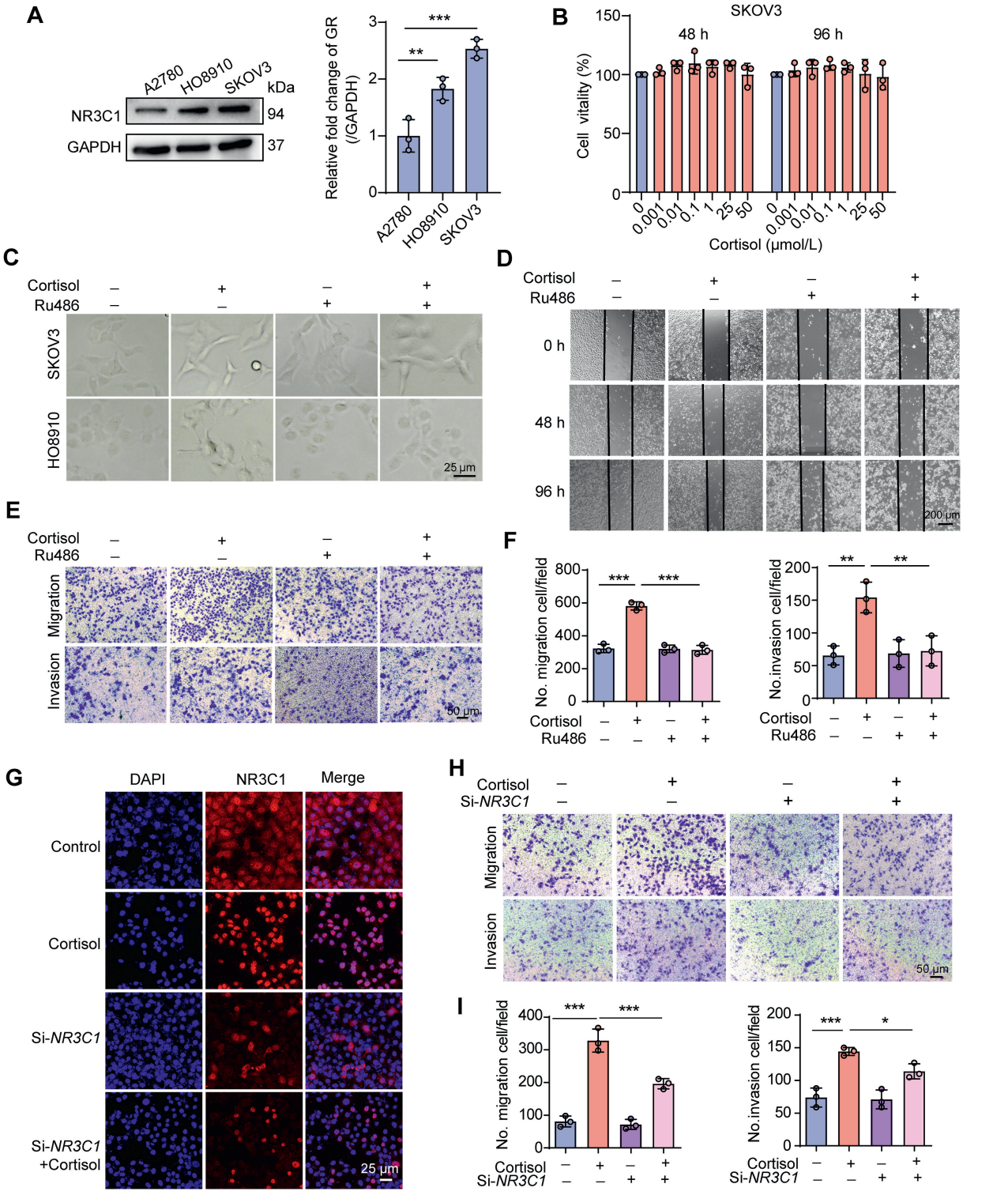


Figure 2 NR3C1 activation contributes to the invasion and migration of OT *in vitro*. (A) NR3C1 expression of SKOV3, HO8910, and A2780 cells was detected by Western blot ($n = 3$). (B) Cell growth of SKOV3 treated with cortisol for 48 and 96 h was detected by MTT ($n = 3$). (C) Cellular morphology of SKOV3 and HO8910 cells treated with cortisol or Ru486 for 48 h was observed by microscope ($n = 3$). (D) Cell migration of SKOV3 cells treated with cortisol or Ru486 for 48 and 96 h were detected by wound healing ($n = 3$). (E, F) Invasion and migration of SKOV3 cells treated with cortisol or Ru486 for 24 h were detected by the Transwell method ($n = 3$). (G) The effect of NR3C1 activation in SKOV3 cells treated with cortisol or si*NR3C1* was observed by immunofluorescence ($n = 3$). (H, I) Invasion and migration of SKOV3 cells treated with CORT or si*NR3C1* for 24 h were detected by the Transwell method ($n = 3$). All data represent mean ± SD. $^{*}P < 0.05$, $^{**}P < 0.01$, $^{***}P < 0.001$, by one-way ANOVA with Tukey.

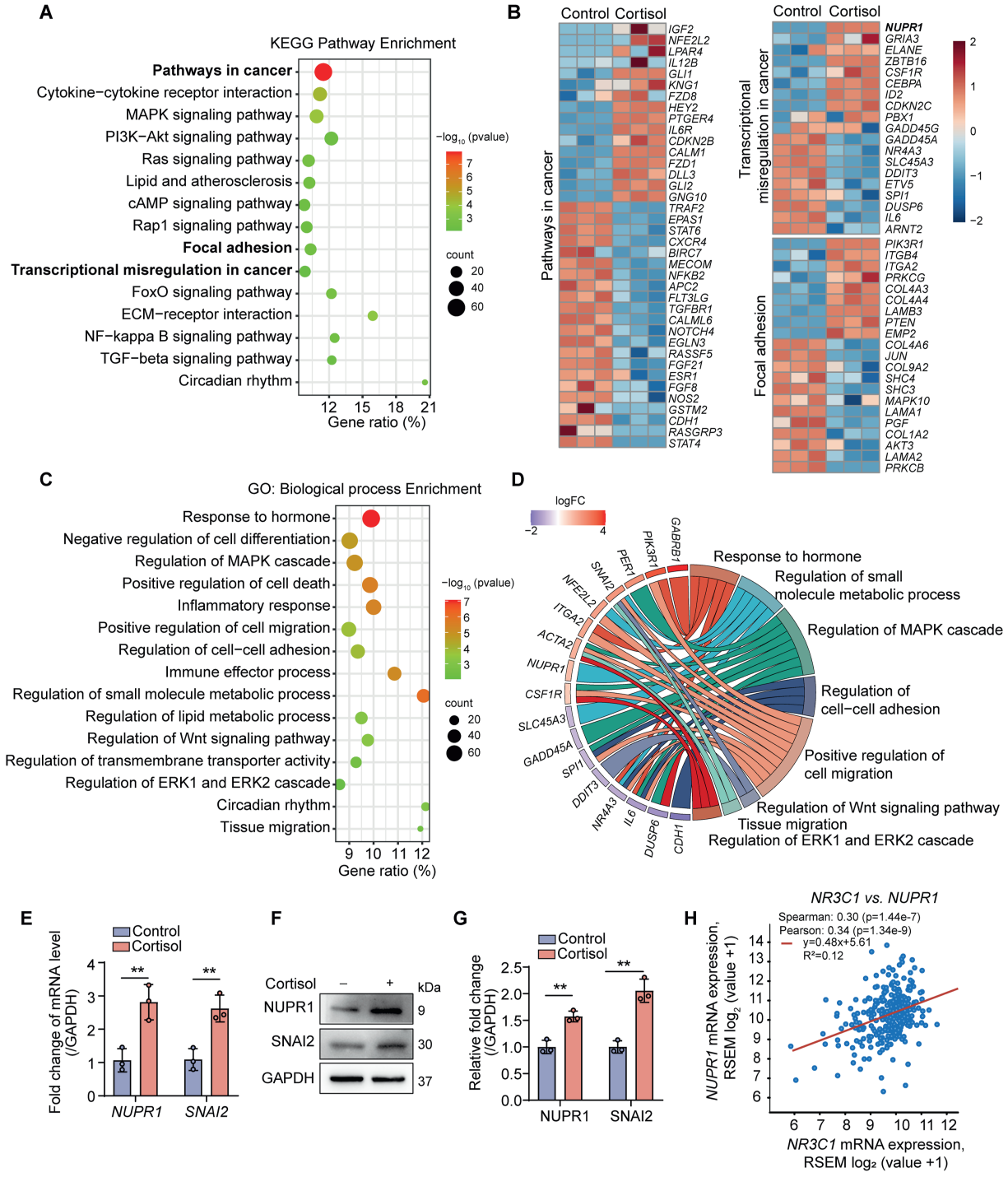


Figure 3 NUPR1 expression is highly correlated with GC-induced NR3C1 activation. (A) The KEGG pathway enrichment analysis of differential genes in SKOV3 cells treated with or without cortisol ($n = 3$). (B) Expression profile of differential genes related to pathways in cancer, transcriptional mis-regulation in cancer, and focal adhesion in SKOV3 cells ($n = 3$). (C) The biological process enrichment analysis of differential genes in SKOV3 cells treated with or without cortisol ($n = 3$). (D) The GO chord indicates overlapped the differential genes across the biological process. (E−G) The mRNA and protein levels of NUPR1 and SNAI2 in SKOV3 cells treated with si*NR3C1* for 48 h were analyzed ($n = 3$). (H) Correlation of *NR3C1* mRNA level and *NUPR1* mRNA level in human ovarian cancer samples (TCGA PanCancer Atlas Studies, cBioportal). mRNA level was batch normalized from Illumina HiSeq_RNASeqV2 and shown as $\log_2$ (RSEM + 1). $R^2 = 0.12$, Spearman correlation. All data represent mean ± SD. $^{**}P < 0.01$, by independent-samples *t*-test (for E and G).

results indicate that NURP1 may be responsible for GC-promoted EMT in OT.

3.4. *NR3C1-dependent mediated NUPR1 transcription is essential for OT metastasis*

To investigate the potential role of NUPR1 in GC-promoted EMT in OT, si*NUPR1* was employed for silencing the expression of NUPR1 in SKOV3 cells (Fig. 4A−C). As shown in Fig. 4D−F, knockdown of *NUPR1* significantly reduced SNAI2 protein levels while increasing CDH1 levels. Besides, Transwell analysis demonstrated that *NUPR1* knockdown markedly decreased GC-induced invasion of SKOV3 cells (Fig. 4G and H). These above results strongly indicate that NUPR1 is essential for GC-evoked EMT in OT. Given that GC can enhance the transcription of target genes through glucocorticoid receptor elements (GRE) in promoters, we asked whether the effect of GC on NUPR1 expression is linked to direct NR3C1-dependent transcription. *In silico* promoter, analysis identified three possible GRE within a 2 kb region upstream of the *NUPR1* transcription start site (Fig. 4I). To assess whether NR3C1 directly regulates NUPR1 transcription, the promoter region of NUPR1 was cloned into a luciferase reporter. Strikingly, data obtained from the luciferase activity assay discovered that both NR3C1 overexpression and GC treatment at varying concentrations significantly increased NURP1 transcription (Fig. 4J and K). Additionally, ChIP-qPCR analysis confirmed that site 2 (AGATCAGCCTGTCCA) is the key GRE responsible for GC-mediated NUPR1 transcription (Fig. 4L). Taken together, these findings demonstrate that GC leads to direct, NR3C1-dependent transcription of NUPR1, which is indispensable for GC-induced EMT in OT.

3.5. *NR3C1 and NUPR1 expression are associated with the poor prognosis of OT patients*

To confirm the correlation between *NR3C1* and *NUPR1* mRNA and clinical outcome, including overall survival (OS) and PFS, in OT patients, a public database Kaplan−Meier (KM) plotter was employed in this study. Results revealed that high *NR3C1* mRNA expression was significantly correlated to poor OS ($n = 1656$) [HR = 1.17 (1.01−1.36), $P = 0.039$] and PFS ($n = 1435$) [HR = 1.38 (1.19−1.59), $P = 1.8 \times 10^{-5}$] in OT patients (Fig. 5A and B). Similarly, high expression of *NUPR1* mRNA was associated with worse PFS [HR = 1.16 (1.02−1.32), $P = 0.024$] in OT clinical data analysis (Fig. 5C). Subsequently, the protein expression of NR3C1 was measured by IHC in 75 specimens from patients with ovarian tumors, 9 specimens from patients with OC and 5 normal ovarian specimens from patients with uterine fibroids (Fig. 5D, Supporting Information Table S2). As shown in Fig. 5E−H, NR3C1 expression was low or undetectable in normal and OC specimens. However, higher NR3C1 expression was observed in 48 out of 75 OT specimens (64%), and this expression was positively associated with a higher The International Federation of Gynecology and Obstetrics (FIGO) stage in OT specimens (Table S2). Similarly, NUPR1 expression was absent or low in normal and OC specimens, but significantly higher in 44 out of 75 OT specimens (59%) (Fig. 5I and J, Table S2). Logistic regression analysis showed a positive correlation between NR3C1 expression and worse serous subtype, higher FIGO stage and NUPR1 expression (Supporting Information Table S3). Further multivariate logistic analysis determined that NR3C1 dependently correlated with higher FIGO stage and NUPR1 expression in OT patients (Table S3). The above data indicated that both *NR3C1* and *NUPR1* expressions were strongly linked to poor prognosis in OT patients.

4. Discussion

Strong epidemiological evidence suggests that chronic psychological stress promotes tumor development[4], due to the release of hormones triggered by stress-induced activation of the hypothalamic−pituitary−adrenal axis. These hormones are responsible for the re-establishment of homeostasis after physical or environmental challenge[41]. Epidemiological and clinical studies over the past 30 years have provided evidence for a link between the dysregulation of neuroendocrine hormones, in particular catecholamines and GCs, and cancer progression[42,43]. GCs are steroid hormones regulated by circadian rhythm and stress responses. It was reported that the NR3C1−insulin receptor substrate 1 axis controls EMT and metastasis in breast cancers[44]. Gene expression analysis also revealed that estrogen receptor-negative breast tumors with high NR3C1 expression exhibited activation of EMT and adhesion, correlating NR3C1 activation with poor prognosis[45]. NR3C1 expression was found in 88% of ovarian tumors[18], and high NR3C1 expression predicts shorter PFS in OT patients[19], indicating that NR3C1 is essential for OT progression. In our study, in line with previous research, we demonstrated that restraint stress-induced the release of CORT, which activated NR3C1 and accelerated ovarian tumor progression. Treatment with NR3C1 antagonist Ru486 significantly reduced this effect *in vivo*. Furthermore, NR3C1 activation promoted EMT, cell migration, and invasion *in vitro*, all of which could be blocked by either NR3C1 antagonist Ru486 or si*NR3C1*. Overall, these findings underscore the crucial role of NR3C1 activation in ovarian cancer progression.

Upon binding to GCs, NR3C1 translocates to the nucleus and activates the GRE[46], then regulates various processes, including metabolism, immune response, development, tumorigenesis, and tumor progression[47]. However, the exact mechanism by which NR3C1 regulates ovarian cancer progression remains unclear. NR3C1 has been shown to modulate ER activity through direct protein−protein interactions and may require coactivators for its function[27-29]. Conversely, ER can influence NR3C1's transcriptional activity[26], suggesting a bidirectional and intricate relationship between these receptors. Given that ER is implicated in the regulation of NUPR1[30], this association underscores the intricate linkage between NR3C1 and NUPR1, highlighting the potential for cross-regulatory mechanisms within this signaling network. To investigate this, an expression profile chip was conducted and identified NUPR1 as a potential mediator of GC-promoted EMT in OT. NUPR1, also known as p8 or com1, was initially discovered in rat pancreas and has since been implicated in the metastasis and progression of several cancers, including breast, thyroid, brain, and pancreas malignancies[48]. NUPR1 is structurally related to the high-mobility group of transcriptional regulators, which play a key role in stress response and cancer progression[49]. NUPR1 was involved in promoting pancreatic cancer cell survival under metabolic stress[50] and maintaining autolysosomal efflux by activating synaptosome-associated protein 25 transcription in cancer cells[51]. In our study, we demonstrated that NR3C1 activation in response to CORT dramatically upregulated NUPR1 expression in ovarian cells. This effect was blocked by either depletion of NR3C1 or pharmacological inhibition of NR3C1 signaling by its specific

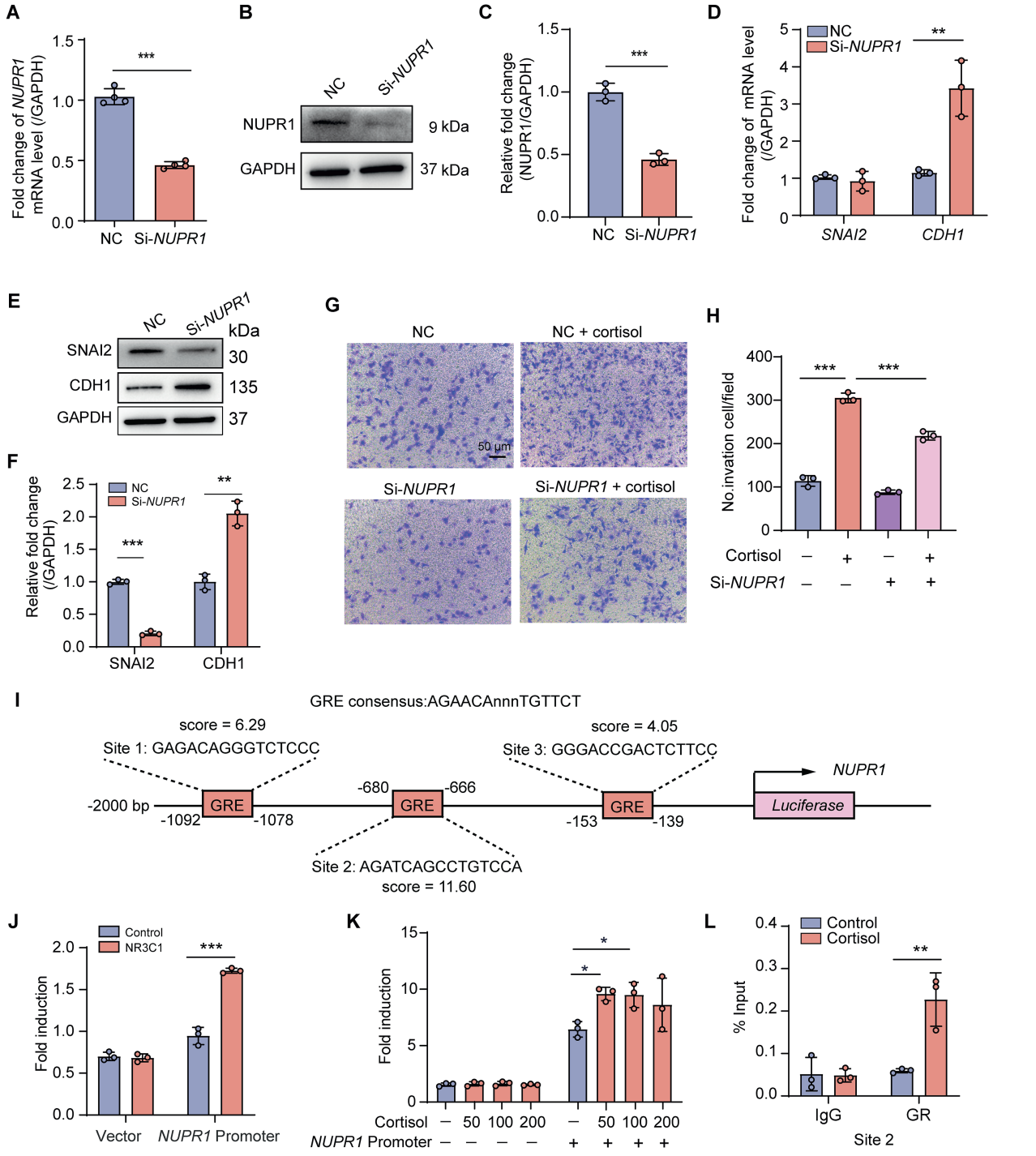


Figure 4 NUPR1 is required for OT metastasis and NR3C1-dependent transcriptional regulated by GC. (A–C) The silencing effect of si*NUPR1* in SKOV3 cells was detected by qRT-PCR and Western blot ($n = 4$). (D–F) The mRNA and protein level of SNAI2 and CDH1 in SKOV3 cells treated with si*NUPR1* for 24 h were detected ($n = 3$). (G, H) The cell invasion of SKOV3 cells treated with CORT/si*NUPR1* for 24 h was detected by the Transwell method ($n = 3$). (I) Schematic map of putative GREs within the 2000 bp region of human NUPR1 promoter. (J, K) Luciferase activities of *NUPR1* were determined in NR3C1 plasmids or cortisol-treated HEK 293 cells ($n = 3$). (L) The enrichment of NR3C1 to the GRE site at *NUPR1* promoter region in HEK293 cells treated with cortisol was analyzed by ChIP assay ($n = 3$). All data represent mean ± SD. $^*P < 0.05$, $^{**}P < 0.01$, $^{***}P < 0.001$, by one-way ANOVA with Tukey.

inhibitor. Moreover, we further demonstrated that NUPR1 knockdown reduced NR3C1 activation-induced SNAI2 overexpression and consequently increased CDH1 level. Consistently, NUPR1 knockdown significantly inhibited the promotion effect of NR3C1 activation on cell migration and invasion ability in ovarian cells. What is surprising is that GC leads a direct, NR3C1-dependent transcription of NUPR1, which is dispensable for GC-induced EMT in OT. These results supported our

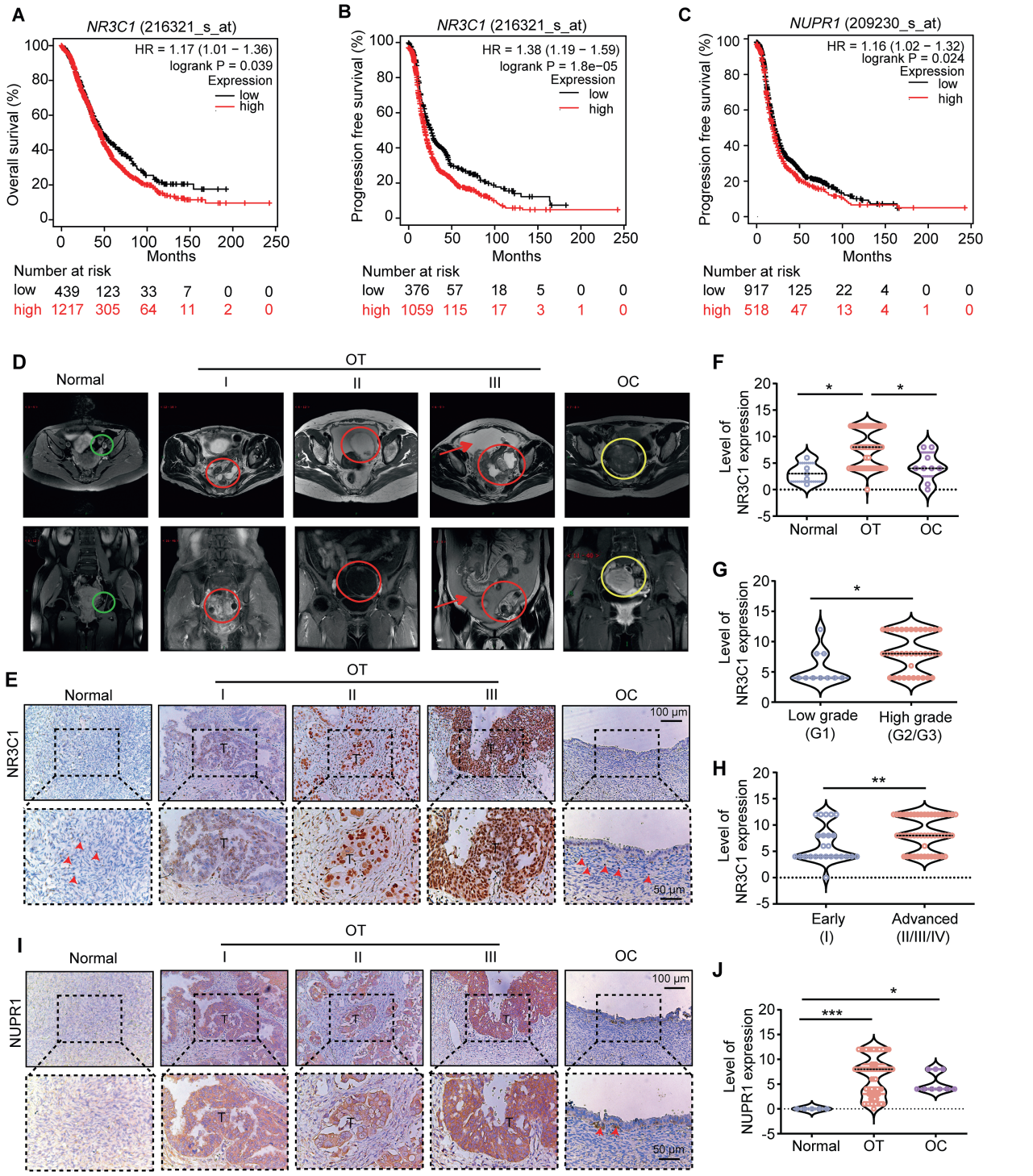


Figure 5 NR3C1 and NUPR1 expression are correlated to the poor prognosis of OT of patients. KM survival analysis for the relationship between survival time, NR3C1 and NUPR1 signatures in OT was performed by using the online tool (http://kmplot.com/analysis/). (A–C) Overall survival ($n = 1656$) and progression-free survival ($n = 1435$) in OT patients. (D) The representative Magnetic Resonance Imaging images in OT ($n = 75$), ovarian endometrial cysts (OC, $n = 9$) and the normal tissues (Normal, $n = 5$) of patients. The green circle indicates the normal ovary of the patient with uterine fibroids; the red circle indicates the OT tissue of I/II/III stage patients; the red arrow indicates the ascites of III stage OT patients; and the yellow circle indicates ovarian cyst tissue of patients with ovarian cyst. (E) Representative IHC staining image and (F) quantification of NR3C1 expression in OT, OC, and normal tissue of patients. "T" indicates the tumor tissue and red arrow indicates NR3C1 positive staining. (G) The level of NR3C1 expression in low grade and high grade of OT tissue. (H) The level of NR3C1 expression in II/III/IV stage and I stage of OT tissue. (I, J) Representative IHC staining image and the quantification of NUPR1 in OT, OC, and normal patients. The "T" indicates tumor tissue and the red arrow indicates NUPR1 positive staining. $*P < 0.05$, $**P < 0.01$, $***P < 0.001$.

hypothesis that NUPR1 might partially mediate the effects of aberrant NR3C1 activation in response to stress.

It is worth noting that our findings, supported by both KM plotter database analysis and our clinical data from OT patients, confirmed that NR3C1 expression is negatively correlated with PFS and OS in OT patients, underscoring the significant role of NR3C1 in OT progression. NR3C1 expression in all the normal and OC specimens was absent or low level, whereas NR3C1 expression in 48/75 (64%) of the OT specimens was significantly elevated. NR3C1 overexpression was positively associated with high-grade serous and higher FIGO stage, both of which are indicators of poor prognosis in OT patients[52]. Similarly, NUPR1 expression was low or undetectable in all the normal and OC specimens, yet it was highly expressed in 59% of OT specimens. Notably, NUPR1 was positively associated with NR3C1 expression in OT specimens and was identified as a dependent prognostic factor for OT patients. Thus, we proposed that NUPR1 might serve as an important downstream effector of NR3C1 in the regulation of ovarian cancer progression. Our study makes a significant contribution to the literature by identifying the NR3C1−NUPR1 axis as a critical signaling pathway mediating the effects of psychological stress on EMT and subsequent OT progression and metastasis. While previous studies have examined the impact of stress on cancer progression, our work is the first to elucidate the specific molecular mechanism involving NR3C1 and NUPR1 in this process. Moreover, our findings extend beyond basic mechanistic insights by providing clinically relevant evidence from OT patient samples, where NR3C1 and NUPR1 overexpression correlate with poor prognosis. This highlights the potential of targeting the NR3C1−NUPR1 axis as a therapeutic strategy, which could offer new avenues for the treatment of stress-exacerbated OT.

5. Conclusions

Taken together, our study provides a novel insight into the mechanism by which chronic stress influences ovarian tumor progression. We identified a novel crosstalk between NR3C1 and NUPR1 signaling. Mechanistically, NR3C1 activation promotes NUPR1 overexpression through direct transcriptional regulation, which in turn increases the expression of SNAI2, one major EMT transcription factor (Fig. 6). More importantly, activated NR3C1 overexpression is positively associated with higher NUPR1 levels in clinical OT samples, with both being correlated with worse prognosis. Our study identified NUPR1 as a potential therapeutic target for the treatment of ovarian tumor progression.

Acknowledgments

This work was supported, in part, by the National Natural Science Foundation of China (Nos. 82374327, 81973718, T2341004, and 82321004), Natural Science Foundation of Guangdong Province (Nos. 2021A1515011297, 2023B1515040016, 2019A15151 10952and 2022A1515012240, China), the Local Innovative and Research Teams Project of Guangdong Pearl River Talents Program (No. 2017BT01Y036, China) and Guangdong Province Universities and Colleges Pearl River Scholar Funded Scheme (2019, China), Guangzhou Basic and Applied Basic Research Foundation (No. 2024A04J4020, China), Science and Technology

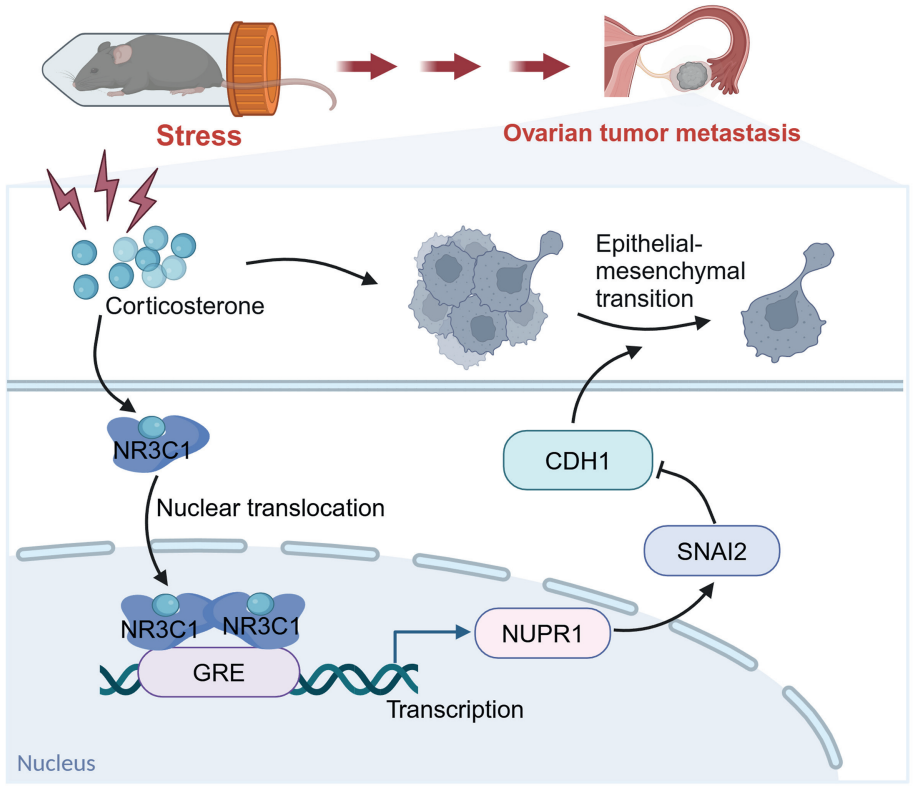


Figure 6 The illustration shows that psychological stress-induced glucocorticoid receptor activation promotes NUPR1 transcription, thereby evoking ovarian tumor metastasis. Created with BioRender.com.

Program of Guangzhou (Nos. 202201020483 and 202201010786, China), Foundation of Guangdong Second Provincial General Hospital (No. 3DA2021015, China), Innovation Team Project of Guangdong Provincial Department of Education (No. 2020KCXTD003, China), Guangdong−Hong Kong−Macao Universities Joint Laboratory for the Internationalization of Traditional Chinese Medicine (No. 2023LSYS002, China), and Guangzhou Key Laboratory of Traditional Chinese Medicine & Disease Susceptibility (No. 2024A03J090, China). We also thank Yinghuan Xiong from the Department of Pathology, Affiliated Hospital of Guangdong Medical University, for providing clinical samples and data.

Author contributions

Bin Liu: Writing − original draft, Methodology, Investigation, Funding acquisition. Wen-Zhe Deng: Methodology, Investigation. Wen-Hua Hu: Methodology, Investigation. Rong-Xi Lu: Methodology, Investigation. Qing-Yu Zhang: Investigation, Funding acquisition. Chen-Feng Gao: Methodology, Investigation. Xiao-Jie Huang: Methodology, Investigation. Wei-Guo Liao: Methodology, Investigation. Jin Gao: Methodology, Investigation. Yang Liu: Investigation. Hiroshi Kurihara: Writing − review & editing. Yi-Fang Li: Writing − review & editing, Supervision. Xu-Hui Zhang: Writing − review & editing, Funding acquisition. Yan-Ping Wu: Writing − review & editing, Funding acquisition, Data curation. Lei Liang: Writing − review & editing, Funding acquisition. Rong-Rong He: Writing − review & editing, Supervision, Project administration, Funding acquisition, Conceptualization.

Conflicts of interests

The authors declare no competing interests.

Appendix A. Supporting information

Supporting information to this article can be found online at https://doi.org/10.1016/j.apsb.2025.04.001.

References

1. Webb PM, Jordan SJ. Epidemiology of epithelial ovarian cancer. *Best Pract Res Clin Obstet Gynaecol* 2017;**41**:3−14.
2. Siegel RL, Miller KD, Jemal A. Cancer statistics, 2020. *CA Cancer J Clin* 2020;**70**:7−30.
3. Markman M. Optimal management of recurrent ovarian cancer. *Int J Gynecol Cancer* 2009;**19**(Suppl 2):S40−3.
4. Armer JS, Clevenger L, Davis LZ, Cuneo M, Thaker PH, Goodheart MJ, et al. Life stress as a risk factor for sustained anxiety and cortisol dysregulation during the first year of survivorship in ovarian cancer. *Cancer* 2018;**124**:3401−8.
5. Liu CL, Liu L, Zhang Y, Dai XZ, Wu H. Prevalence and its associated psychological variables of symptoms of depression and anxiety among ovarian cancer patients in China: a cross-sectional study. *Health Qual Life Outcome* 2017;**15**:161.
6. Obradović MMS, Hamelin B, Manevski N, Couto JP, Sethi A, Coissieux MM, et al. Glucocorticoids promote breast cancer metastasis. *Nature* 2019;**567**:540−4.
7. Antoni MH, Lutgendorf SK, Cole SW, Dhabhar FS, Sephton SE, McDonald PG, et al. The influence of bio-behavioural factors on tumour biology: pathways and mechanisms. *Nat Rev Cancer* 2006;**6**:240−8.
8. Justice A. Review of the effects of stress on cancer in laboratory animals: importance of time of stress application and type of tumor. *Psychol Bull* 1985;**98**:108−38.
9. Qin X, Li J, Wang S, Lv J, Luan F, Liu Y, et al. Serotonin/HTR1E signaling blocks chronic stress-promoted progression of ovarian cancer. *Theranostics* 2021;**11**:6950−65.
10. Nilsson MB, Armaiz-Pena G, Takahashi R, Lin YG, Trevino J, Li Y, et al. Stress hormones regulate interleukin-6 expression by human ovarian carcinoma cells through a Src-dependent mechanism. *J Biol Chem* 2007;**282**:29919−26.
11. Glaser R, Kiecolt-Glaser JK. Stress-induced immune dysfunction: implications for health. *Nat Rev Immunol* 2005;**5**:243−51.
12. Lin XM, Pan MH, Sun J, Wang M, Huang ZH, Wang G, et al. Membrane phospholipid peroxidation promotes loss of dopaminergic neurons in psychological stress-induced Parkinson's disease susceptibility. *Aging Cell* 2023;**22**:e13970.
13. Wu Y, Luo X, Zhou Q, Gong H, Gao H, Liu T, et al. The disbalance of LRP1 and SIRPα by psychological stress dampens the clearance of tumor cells by macrophages. *Acta Pharm Sin B* 2022;**12**:197−209.
14. Biddie SC, Conway-Campbell BL, Lightman SL. Dynamic regulation of glucocorticoid signalling in health and disease. *Rheumatology (Oxford)* 2012;**51**:403−12.
15. Skor MN, Wonder EL, Kocherginsky M, Goyal A, Hall BA, Cai Y, et al. Glucocorticoid receptor antagonism as a novel therapy for triple-negative breast cancer. *Clin Cancer Res* 2013;**19**:6163−72.
16. Zhang C, Kolb A, Büchler P, Cato AC, Mattern J, Rittgen W, et al. Corticosteroid co-treatment induces resistance to chemotherapy in surgical resections, xenografts and established cell lines of pancreatic cancer. *BMC Cancer* 2006;**6**:61.
17. Stringer-Reasor EM, Baker GM, Skor MN, Kocherginsky M, Lengyel E, Fleming GF, et al. Glucocorticoid receptor activation inhibits chemotherapy-induced cell death in high-grade serous ovarian carcinoma. *Gynecol Oncol* 2015;**138**:656−62.
18. Galli MC, De Giovanni C, Nicoletti G, Grilli S, Nanni P, Prodi G, et al. The occurrence of multiple steroid hormone receptors in disease-free and neoplastic human ovary. *Cancer* 1981;**47**:1297−302.
19. Veneris JT, Darcy KM, Mhawech-Fauceglia P, Tian C, Lengyel E, Lastra RR, et al. High glucocorticoid receptor expression predicts short progression-free survival in ovarian cancer. *Gynecol Oncol* 2017;**146**:153−60.
20. Krebs AM, Mitschke J, Lasierra Losada M, Schmalhofer O, Boerries M, Busch H, et al. The EMT-activator Zeb1 is a key factor for cell plasticity and promotes metastasis in pancreatic cancer. *Nat Cell Biol* 2017;**19**:518−29.
21. Chen T, Liu G, Chen S, Zhang F, Ma S, Bai Y, et al. Natural product mediated mesenchymal−epithelial remodeling by covalently binding ENO1 to degrade m6A modified β-catenin mRNA. *Acta Pharm Sin B* 2025;**15**:467−83.
22. Chang L, Hu Y, Fu Y, Zhou T, You J, Du J, et al. Targeting slug-mediated non-canonical activation of c-Met to overcome chemoresistance in metastatic ovarian cancer cells. *Acta Pharm Sin B* 2019;**9**:484−95.
23. Zheng H, Li W, Wang Y, Xie T, Cai Y, Wang Z, et al. miR-23a inhibits E-cadherin expression and is regulated by AP-1 and NFAT4 complex during Fas-induced EMT in gastrointestinal cancer. *Carcinogenesis* 2014;**35**:173−83.
24. Park KS, Dubon MJ, Gumbiner BM. N-cadherin mediates the migration of MCF-10A cells undergoing bone morphogenetic protein 4-mediated epithelial mesenchymal transition. *Tumour Biol* 2015;**36**:3549−56.
25. Wu J, Zhang Y, Cheng R, Gong W, Ding T, Zhai Q, et al. Expression of epithelial−mesenchymal transition regulators TWIST, SLUG and SNAIL in follicular thyroid tumours may relate to widely invasive, poorly differentiated and distant metastasis. *Histopathology* 2019;**74**:780−91.
26. Vahrenkamp JM, Yang CH, Rodriguez AC, Almomen A, Berrett KC, Trujillo AN, et al. Clinical and genomic crosstalk between

glucocorticoid receptor and estrogen receptor α in endometrial cancer. *Cell Rep* 2018;**22**:2995−3005.
27. Cvoro A, Yuan C, Paruthiyil S, Miller OH, Yamamoto KR, Leitman DC. Cross talk between glucocorticoid and estrogen receptors occurs at a subset of proinflammatory genes. *J Immunol* 2011;**186**:4354−60.
28. Karmakar S, Jin Y, Nagaich AK. Interaction of glucocorticoid receptor (GR) with estrogen receptor (ER) α and activator protein 1 (AP1) in dexamethasone-mediated interference of ERα activity. *J Biol Chem* 2013;**288**:24020−34.
29. Bolt MJ, Stossi F, Newberg JY, Orjalo A, Johansson HE, Mancini MA. Coactivators enable glucocorticoid receptor recruitment to fine-tune estrogen receptor transcriptional responses. *Nucleic Acids Res* 2013; **41**:4036−48.
30. Wang L, Sun J, Yin Y, Sun Y, Ma J, Zhou R, et al. Transcriptional coregualtor NUPR1 maintains tamoxifen resistance in breast cancer cells. *Cell Death Dis* 2021;**12**:149.
31. Mallo GV, Fiedler F, Calvo EL, Ortiz EM, Vasseur S, Keim V, et al. Cloning and expression of the rat p8 cDNA, a new gene activated in pancreas during the acute phase of pancreatitis, pancreatic development, and regeneration, and which promotes cellular growth. *J Biol Chem* 1997;**272**:32360−9.
32. Mansour SMA, Ali SA, Nofal S, Soror SH. Targeting NUPR1 for cancer treatment: a risky endeavor. *Curr Cancer Drug Targets* 2020;**20**:768−78.
33. Lan W, Santofimia P, Swayden M, Xia Y, Zhou Z, Audebert S, et al. ZZW-115-dependent inhibition of NUPR1 nuclear translocation sensitizes cancer cells to genotoxic agents. *JCI Insight* 2020;**5**:e138117.
34. Santofimia P, Xia Y, Peng L, Velázquez A, Abián O, Lan W, et al. Targeting the stress-induced protein NUPR1 to treat pancreatic adenocarcinoma. *Cells* 2019;**8**:1453.
35. Terenina E, Fabre S, Bonnet A, Monniaux D, Robert-Granié C, SanCristobal M, et al. Differentially expressed genes and gene networks involved in pig ovarian follicular atresia. *Physiol Genom* 2017; **49**:67−80.
36. Cho S, Sun Y, Soisson AP, Dodson MK, Peterson CM, Jarboe EA, et al. Characterization and evaluation of pre-clinical suitability of a syngeneic orthotopic mouse ovarian cancer model. *Anticancer Res* 2013;**33**:1317−24.
37. Luo Z, Liu LF, Jiang YN, Tang LP, Li W, Ouyang SH, et al. Novel insights into stress-induced susceptibility to influenza: corticosterone impacts interferon-β responses by Mfn2-mediated ubiquitin degradation of MAVS. *Signal Transduct Targeted Ther* 2020;**5**:202.
38. Mu N, Gu J, Huang T, Zhang C, Shu Z, Li M, et al. A novel NF-κB/YY1/microRNA-10a regulatory circuit in fibroblast-like synoviocytes regulates inflammation in rheumatoid arthritis. *Sci Rep* 2016;**6**:20059.
39. Sun R, Wu J, Chen Y, Lu M, Zhang S, Lu D, et al. Down regulation of thrombospondin2 predicts poor prognosis in patients with gastric cancer. *Mol Cancer* 2014;**13**:225.
40. Heinonen PK, Tontti K, Koivula T, Pystynen P. Tumour-associated antigen CA 125 in patients with ovarian cancer. *Br J Obstet Gynaecol* 1985;**92**:528−31.
41. Herman JP, McKlveen JM, Ghosal S, Kopp B, Wulsin A, Makinson R, et al. Regulation of the hypothalamic-pituitary-adrenocortical stress response. *Compr Physiol* 2016;**6**:603−21.
42. Moreno-Smith M, Lutgendorf SK, Sood AK. Impact of stress on cancer metastasis. *Future Oncol* 2010;**6**:1863−81.
43. Feng Z, Liu L, Zhang C, Zheng T, Wang J, Lin M, et al. Chronic restraint stress attenuates p53 function and promotes tumorigenesis. *Proc Natl Acad Sci U S A* 2012;**109**:7013−8.
44. Shi W, Wang D, Yuan X, Liu Y, Guo X, Li J, et al. Glucocorticoid receptor−IRS-1 axis controls EMT and the metastasis of breast cancers. *J Mol Cell Biol* 2019;**11**:1042−55.
45. Pan D, Kocherginsky M, Conzen SD. Activation of the glucocorticoid receptor is associated with poor prognosis in estrogen receptor-negative breast cancer. *Cancer Res* 2011;**71**:6360−70.
46. Slater EP, Rabenau O, Karin M, Baxter JD, Beato M. Glucocorticoid receptor binding and activation of a heterologous promoter by dexamethasone by the first intron of the human growth hormone gene. *Mol Cell Biol* 1985;**5**:2984−92.
47. Kadmiel M, Cidlowski JA. Glucocorticoid receptor signaling in health and disease. *Trends Pharmacol Sci* 2013;**34**:518−30.
48. Chowdhury UR, Samant RS, Fodstad O, Shevde LA. Emerging role of nuclear protein 1 (NUPR1) in cancer biology. *Cancer Metastasis Rev* 2009;**28**:225−32.
49. Cano CE, Hamidi T, Sandi MJ, Iovanna JL. Nupr1: the Swiss-knife of cancer. *J Cell Physiol* 2011;**226**:1439−43.
50. Hamidi T, Cano CE, Grasso D, Garcia MN, Sandi MJ, Calvo EL, et al. Nupr1-aurora kinase A pathway provides protection against metabolic stress-mediated autophagic-associated cell death. *Clin Cancer Res* 2012;**18**:5234−46.
51. Mu Y, Yan X, Li D, Zhao D, Wang L, Wang X, et al. NUPR1 maintains autolysosomal efflux by activating SNAP25 transcription in cancer cells. *Autophagy* 2018;**14**:654−70.
52. Chen GM, Kannan L, Geistlinger L, Kofia V, Safikhani Z, Gendoo DMA, et al. Consensus on molecular subtypes of high-grade serous ovarian carcinoma. *Clin Cancer Res* 2018;**24**:5037−47.